Electronic Supplementary Material (ESI) for RSC Advances.
This journal is © The Royal Society of Chemistry 2017

Electronic Supplementary Information

Conversion of supramolecular organic framework to uranyl-organic coordination complex: a new "matrix-free" strategy for highly efficient capture of uranium

Bo Li[a], Lei Wang[a], Yang Li[a], Dongqi Wang[b], Rui Wen[a], Xinghua Guo[a], Shoujian Li[*a], Lijian Ma[*a] and Yin Tian[*c]

[a]College of Chemistry, Sichuan University, Key Laboratory of Radiation Physics & Technology, Ministry of Education, No 29 Wangjiang Road, Chengdu, 610064, P. R. China. Fax: 86 28 85412907; Tel: 86 28 85412329; E-mail: sjli000616@scu.edu.cn and ma.lj@hotmail.com

[b] CAS Key Laboratory of Nuclear Radiation and Nuclear Energy Techniques, and Institute of High Energy Physics, Chinese Academy of Sciences, Beijing, 100049, China.

[c]Southwestern Institute of Physics, Chengdu 610041, People's Republic of China. E-mail: tianyin@swip.ac.cn

*Corresponding author.

Tel.: +86 28 85412329

Fax: +86 28 85412907

E-mail address: sjli000616@scu.edu.cn (S. Li).

(b) $UO_2(NO_3)_2(H_2O)_2$ by DFT calculations.

28) Reference

Section S1. Preparation of HSOF, UOCC and LaOCC.

Briefly, MA (0.506 g, 4 mmol) and TMA (0.211 g, 1 mmol) were dissolved in 150 ml of hot distilled water respectively. After complete dissolution, the hot aqueous solution of TMA was then added dropwise into the hot aqueous solution of MA. After a time a perfectly white, flocculent precipitate began to form during the self-assembly process. The as-prepared material was washed thoroughly with deionized water, ethanol and acetone alternately. The final white solid powder (Fig. S1a†) was dried in a vacuum oven for 12 h at 323 K for standby application and denoted as HSOF. Detail experimental parameters (reaction time, temperature, molar ratio, and so on) and extraction results were listed in Table S1†. The U(VI)-, La(III)- loaded HSOF samples obtained in pure uranium or lanthanum solution ($C_0 = 300$ mg L^{-1}, $v = 25$ mL, $\omega = 10$ mg, $T = 298$ K) with three parallel samples were washed thoroughly with deionized water until the filtrate was nearly neutral followed by drying in a vacuum oven at 323 K for 12 h. The final prepared materials were donated as UOCC and LaOCC.

Section S2. Preparation of U(VI), La(III), Co(II) and multi-ion stock solution, test solution.

The stock solution of uranyl nitrate (~1000 mg L^{-1}) or lanthanum nitrate (~1000 mg L^{-1}) or cobalt (~1000 mg L^{-1}) were prepared by dissolving appropriate amounts of $UO_2(NO_3)_2 \cdot 6H_2O$ or $La(NO_3)_3 \cdot 6H_2O$ or $Co(NO_3)_2 \cdot 6H_2O$ in nitric acid aqueous solution. The working solution (100–300 mg L^{-1}) was prepared by diluting the stock solution with deionized water to demanded concentrations, and adjusted to desired pH value using a negligible volume of dilute solution of sodium hydroxide and/or nitric acid when needed. Similarly, the multi-ion solution containing 11 competing ions (La^{3+}, Sm^{3+}, Nd^{3+}, Gd^{3+}, Ce^{3+}, Ba^{2+}, Sr^{2+}, Mn^{2+}, Co^{2+}, Ni^{2+}, Zn^{2+}, listed in Table S4†) selected mainly based on the composition of a typical nuclear power reactor effluent,[1] which was prepared by dissolving the metal oxides or nitrates in nitric acid aqueous solution with the each metal concentration of about 1.00 mmol L^{-1}.

Section S3. Batch extraction experiments

10 mg of HSOF was added into a 50 mL Erlenmeyer flasks along with 25 mL of either pure U(VI) or La(III) or Co(II) solution or a stimulated weak acid multi-cations competing system

with designed metal ion concentration and pH value. All samples were shaken for a certain time (*t*, min) at specified temperatures (*T*, K). Then the solid was separated from supernatant by centrifugation, and the concentrations of metal ions in the supernatant, before and after extraction, were determined by ICP-AES. All samples were tested at least twice during ICP-AES measurements, the operating parameters for the ICP-AES are described in Table S5†. Low concentration of U(VI) was determined by the laser fluorescence analyzer of trace uranium (WGJ-III, China). All glassware was soaked in 10.0 wt% HNO_3 solution for 12 h before used to remove any metal impurities which might be adsorbed on the walls of glassware. All tests were carried out at least in duplicates.

Section S4. Kinetic studies

Three different kinetic models, namely pseudo-first-order, pseudo-second-order model and intraparticle diffusion model were employed to evaluate the controlling mechanism of the extraction process. The linear forms of the three models can be expressed by the following equations. (1)-(3) respectively,[2, 3]

$$\ln(q_{\mathrm{e}} - q_t) = \ln q_{\mathrm{e}} - k_1 t \qquad (1)$$

$$\frac{t}{q_t} = \frac{1}{k_2 q_{\mathrm{e}}^2} + \frac{1}{q_{\mathrm{e}}}\, t \qquad (2)$$

$$q_t = k_{\mathrm{int}} t^{0.5} + C \qquad (3)$$

where q_{t} refers to the amount of U(VI) adsorbed (mg g^{-1}) at any time *t*, k_1 (min^{-1}) and k_2 (g mg^{-1} min^{-1}) are the pseudo-first-order and the pseudo-second-order rate constants, respectively. k_{int} (mg g^{-1} $min^{-1/2}$) is the intraparticle diffusion rate constant, and *C* (mg g^{-1}) is the constant proportional to the extent of boundary layer thickness.

For Eqs. (1)−(3), linear plots of ln ($q_{\mathrm{e}} - q_{\mathrm{t}}$) vs. *t*, t/q_{t} vs. *t* and q_{t} vs. $t^{1/2}$ are given respectively in Fig. S8† (a)−(c). The values of constants in Eqs, (1)−(3) are shown in Table S7†.

Section S5 Isotherm studies

The extraction data were fitted using the three types of frequently used isotherms, namely Langmuir, Freundlich and Dubinin and Radushkevich (D–R) isotherm, to further understand the extraction performance of HSOF toward U(VI) .

The linear equation of the Langmuir extraction model is given in Eq. (4).[4, 5]

$$\frac{C_\mathrm{e}}{q_\mathrm{e}} = \frac{1}{q_L q_L} + \frac{1}{q_L} C_\mathrm{e} \qquad (4)$$

$$R_L = \frac{1}{1 + b_L C_0} \qquad (5)$$

where b_L is the Langmuir constant related to the energy of extraction (L mg^{-1}) and q_L is the maximum extraction capacity (mg g^{-1}) .

The linear equation of the Freundlich isotherm is given in Eq. (6).[4]

$$\ln q_\mathrm{e} = \ln K_\mathrm{F} + \frac{1}{\mathrm{n}_F} \ln C_\mathrm{e} \qquad (6)$$

where K_F [mg g^{-1} (L $\mathrm{mg})^{1/\mathrm{n}}$] and n_F are characteristic constants related to the relative extraction capacity of the extractant and the intensity of extraction, respectively. The q_L, b_L, K_F, n_F values and the linear regression correlations for Langmuir (R^2), Freundlich (R^2) were listed in Table S9†. The linear forms of the Langmuir and Freundlich equations were also shown in Fig. S9 (a) and (b) †.

On the comparison of the R^2 values given in Table S9†, we could be concluded that Langmuir equation represents a better fit to the experimental data than the Freundlich equation. It was suggested that the present extraction process probably dominated by a monolayer extraction rather than a multilayer one. It was revealed that the energy distribution for the active sites on HSOF was of essentially a uniform type, rather than of the exponential type. Theoretical saturated extraction capacities of Langmuir (454.5 mg g^{-1}) isotherm are very close to experimental data (444.0 mg g^{-1}). Which was suggested the more exact description of the process by Langmuir. The value of R_L (Fig. S10†) indicated the process to be favorable since R_L was between 0 and 1, and was in agreement with Freundlich model in which the values of n_F greater than 1 also showed the favorable nature of extraction.

The mean adsorption energy (E) calculated from the D–R isotherm can provide more important information about the chemical or physical properties. The D–R isotherm is given in Eq. (7). [6]

$$\ln q_{\mathrm{e}} = \ln q_{\mathrm{DR}} - \beta\varepsilon^2 \qquad (7)$$

where q_{DR} (mg g^{-1}) is the D–R extraction capacity, β (mol^2 J^{-2}) is a constant related to the extraction energy and ε is the Polanyi potential. ε is calculated with the following Eq. (8).

$$\varepsilon = RT\ln\left(1+\frac{1}{c_{\mathrm{e}}}\right) \qquad (8)$$

where R is the gas constant (8.314 J mol^{-1} K^{-1}) and T is the temperature (K).

The values of q_{DL} and β were calculated from the intercept and slope of the lnq_{e} versus ε^2 plots given in Fig. S10c† and listed in Table S9†. The mean extraction energy (E, kJ mol^{-1}) could be obtained from the β value of D–R isotherms using the following Eq. (9).

$$E = \frac{1}{\sqrt{-2\beta}} \qquad (9)$$

In this study, E value was calculated to be 31.45 kJ mol^{-1}, which is bigger than the energy range of adsorption reactions, 8–16 kJ mol^{-1}. The type of extraction of uranium onto the HSOF was defined as chemical adsorption.[7, 8]

Table S1 Different experimental conditions for the preparation of the HSOF and its extraction capacity and selectivity (S_U) toward uranium [a].

Number	*MA* （*g*）	*TMA* （*g*）	*T* (K)	DR[b] (mL min^{-1})	q_{tol} (mmolg^{-1})	q_u (mmolg^{-1})	S_u(%)
1	0.126	0.21	60	10	2.57	1.27	49.0
2	0.252	0.42	60	30	2.29	1.26	55.0
3	0.54	0.8	60	60	2.11	1.26	60.0
4	0.126	0.8	80	30	2.45	1.27	52.0
5	0.252	0.21	80	60	2.34	1.28	55.0
6	0.54	0.42	80	10	2.43	1.29	53.0
7	0.126	0.42	100	60	2.61	1.28	49.0
8	0.252	0.8	100	10	2.47	1.26	51.0
9	0.54	0.21	100	30	1.76	1.32	75.0

[a] Extraction conditions: $C_0 \approx 0.5$ mmol L^{-1} all cations, pH = 4.5, $t = 120$ min, $V = 25$ mL, $T = 298$ K, and $\omega = 10$ mg.

[b] Dropping rate

Table S2 Elemental analyses of MA, TMA, and HSOF.

Sample	C (at %)	N (at %)	O (at %)	H (at %)
MA	28.6	66.7	—	4.7
TMA	51.4	—	45.7	2.9
HSOF	32.0	34.2	28.5	5.3
Calculated[a]	33.7	31.5	29.9	4.9

[a]: Calculated from the ratio of MA: TMA = 1: 2

Table S3 Atom percent of UOCC by XPS analysis.

Sample	C (at %)	N (at %)	O (at %)	U (at %)
UOCC	33.9	12.0	24.8	29.3
Calculated[a]	30.1	10.0	27.5	29.2

[a]: Calculated from the ratio of MA: TMA: UO_2^{2+} = 1: 2: 1

Table S4 Compositions of the multi-ions aqueous systems containing 12 cations.

Coexistent ion	Added as	Reagent purity
UO_2^{2+}	$UO_2(NO_3)_2 \cdot 6H_2O$	Standard reagent
La^{3+}	$La(NO_3)_3 \cdot 6H_2O$	99.9% metal basis
Ce^{3+}	$Ce(NO_3)_3 \cdot 6H_2O$	99.99% metal basis
Nd^{3+}	$Nd(NO_3)_3 \cdot 6H_2O$	AR
Sm^{3+}	$Sm(NO_3)_3 \cdot 6H_2O$	AR
Gd^{3+}	$Gd(NO_3)_3 \cdot 6H_2O$	AR
Mn^{2+}	MnO	99.5%
Co^{2+}	$Co(NO_3)_2 \cdot 6H_2O$	99.99% metal basis
Ni^{2+}	$Ni(NO_3)_2 \cdot 6H_2O$	Spectrum pure
Zn^{2+}	$Zn(NO_3)_2 \cdot 6H_2O$	99.99% metal basis
Sr^{2+}	$Sr(NO_3)_2$	99.99% metal basis
Ba^{2+}	$Ba(NO_3)_2$	99.999%

Table S5 Operating parameters for ICP-AES.

Radio-frequency (RF) power (W)	1150
Carrier argon flow rate (L min^{-1})	0.6
Auxiliary argon flow rate (L min^{-1})	Low
Coolant argon flow rate (min^{-1})	14
Nebulizer gas (PSI)	27
Integration time (s)	25
Wavelength (nm)	U 385.9；Gd 342.2 Sm 442.4；Nd 430.4 La 333.7；Ce 413.3 Ni 231.6；Zn 213.8 Co 228.6；Ba 493.4 Sr 407.7；Mn 257.6

Table S6 Comparison of uranium extraction equilibrium time of various extractants

Extractant	pH	C_0 (mmol L^{-1})	q_u (mg g^{-1})	EET[a]	Ref
MPCOF[b]	1.5	0.45	142	41 d	9
$Mg(OH)_2$	-	0.17	30	15 h	10
MOF-76	3.0	0.59	280	5 h	11
MIL-deta[c]	5.5	0.42	230	2 h	12
HTC-Sal[d]	4.3	0.5	126	30 min	13
NP10[e]	6.9	0.55	90	30 min	14
HTC-acy[f]	4.5	0.84	220	<30 min	15
DIMS[g]	5.0	0.56	80	~10 min	16
HSOF	4.5	0.84	422	<10 min	This work

[a]Extraction equilibrium time. [b]Microporous phosphazene-based covalent organic framework. [c]Diethylenetriamine-functionalized chromium-based MOF. [d]Salicylideneimine-functionalized hydrothermal carbon. [e]Phosphonate-functionalized mesoporous silica. [f]5-azacytosine-functionalized hydrothermal carbon. [g]Dihydroimidazole-functionalized SBA-15.

Table S7. Kinetic parameters for the U(VI) extraction onto HSOF

q_e (exp) (mg g^{-1})	pseudo-first-order equation			pseudo-second-order equation		
	$q_{e,cal}$ (mg g^{-1})	k_1 (min^{-1})	R^2	$q_{e,cal}$ (mg g^{-1})	k_2 (g mg^{-1} min^{-1})	R^2
422.0	39.88	0.0325	0.8234	414.9	0.00241	0.9997

Intrapaticle diffusion

k_{int} (mg g^{-1} min$^{-(1/2)}$)	C mg g^{-1}	R^2
9.226	383.7	0.9827

Table S8 Uranium removal efficiency onto HSOF at different uranium concentration (20−130 mg L^{-1}).

C_o (mg L^{-1})	q_e (mg g^{-1})	U removal (%)
22.7	56.3	99.7
66	164.6	99.9
97	242.3	99.8
130	323.3	>99.9
160	372.4	92.3

Table S9 Isotherm parameters for the uranium(VI) extraction onto HSOF.

T (K)	q_e (mg g^{-1})	Langmuir isotherm			Freundlich isotherm		
		q_L (mg g^{-1})	b_L (L mg^{-1})	R^2	K_F [mg g^{-1} (L mg)$^{1/n}$]	n_F	R^2
298.15	444.0	454.5	0.274	0.998	322.5	15.6	0.995

D-R isotherm			
q_{DR} (mg g^{-1})	β （mol^2 kJ^{-2}）	E (kJ mol^{-1})	R^2
563.4	0.000506	31.45	0.992

Table S10 The Wiberg bond indices (WBIs) of U–O Bonds and selected atom charges (Q) obtained by natural bond orbital (NBO) analysis.[a]

Species	U–$O_{carboxyl}$	U–N_L	U–O_{water}	U–$O_{nitrate}$	Q(U)	Q(O_L)	Q(N_L)
$[UO_2(H_2O)_5]^{2+}$			0.417		1.882		
$UO_2(NO_3)_2(H_2O)_2$			0.404	0.434	1.584		
UOCC-1	0.456		0.398		1.563	−0.652	
UOCC-2	0.458	0.386			1.521	−0.643	−0.732

[a] The $O_{carboxyl}$ and N_L are the coordinated oxygen and nitrogen atoms in UOCC

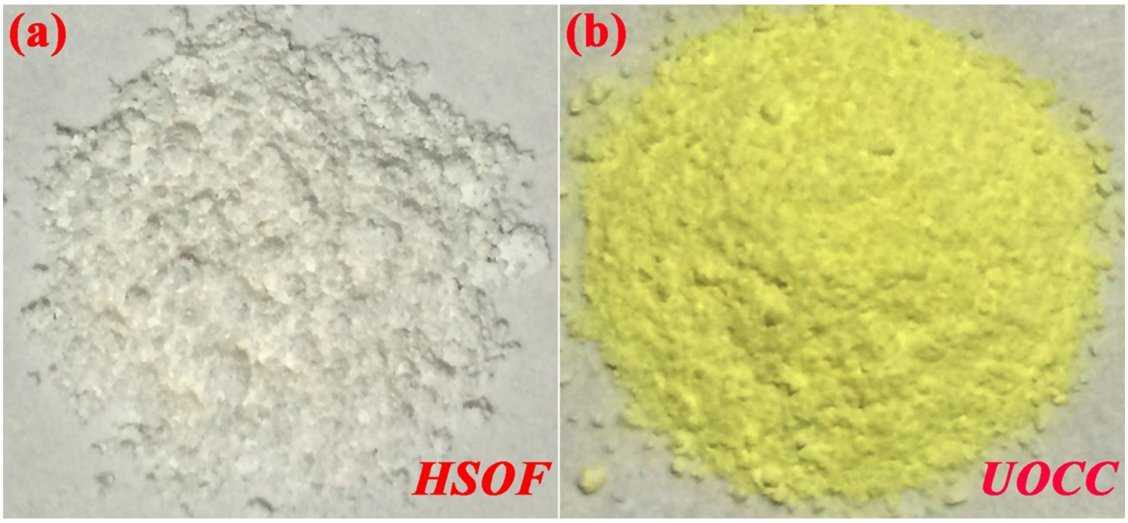

Fig. S1 Photograph images of (a) HSOF, (b) UOCC.

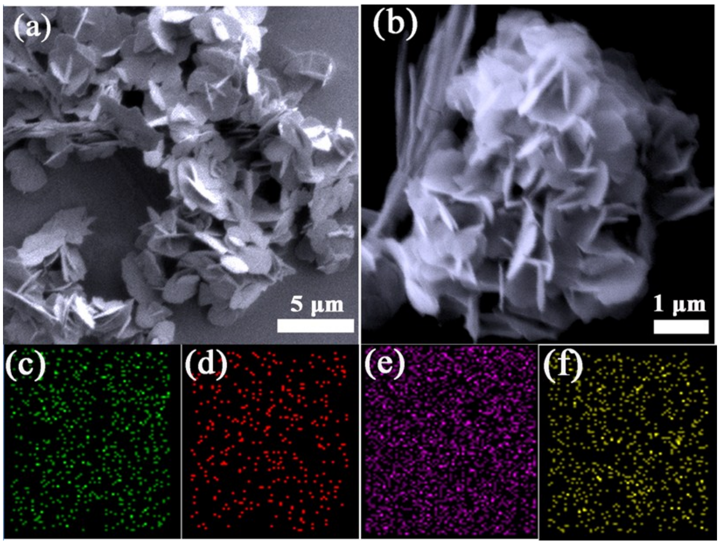

Fig. S2 SEM images of (a) UOCC (after uranium capture by HSOF in pure uranium solution). (b) UOCC (after uranium capture by HSOF in multi-ions systems). Elemental EDX mapping images of UOCC: (c) C, (d) N, (e) O, and (f) U.

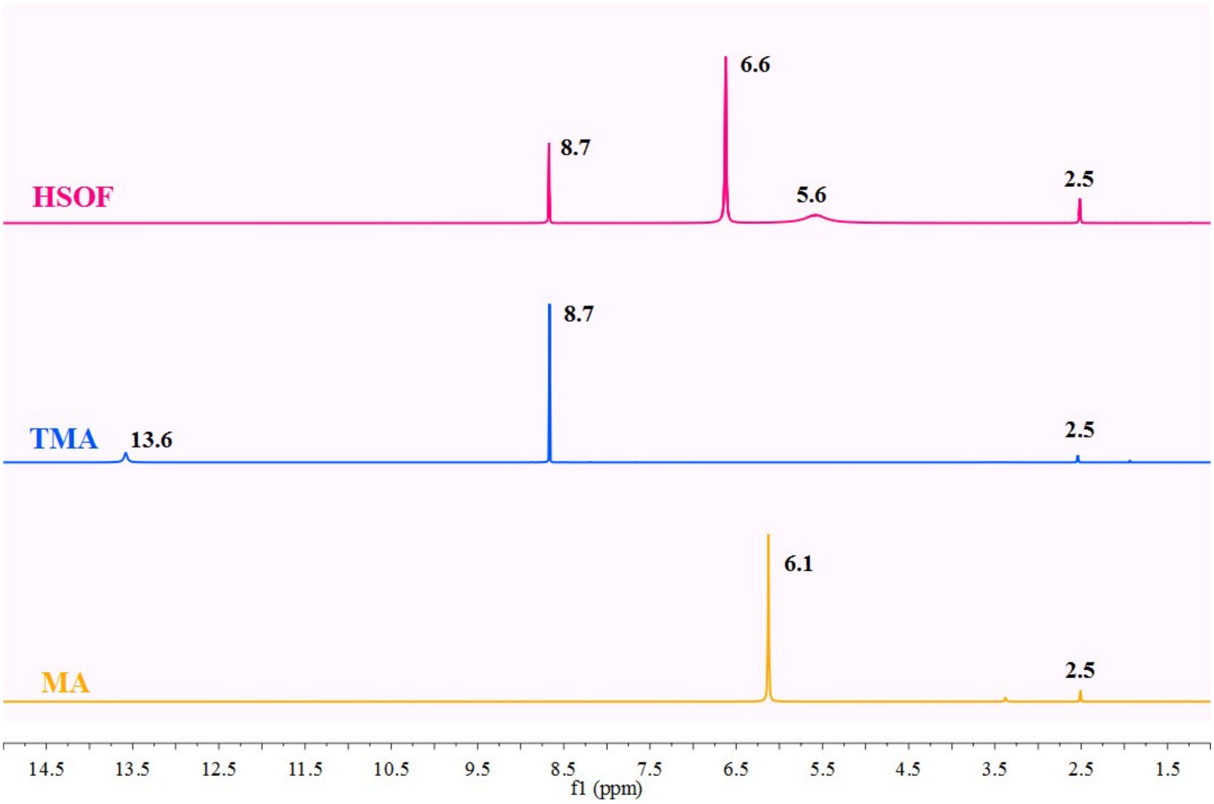

Fig. S3 ^{1}H NMR signal of MA, TMA and HSOF in DMSO.

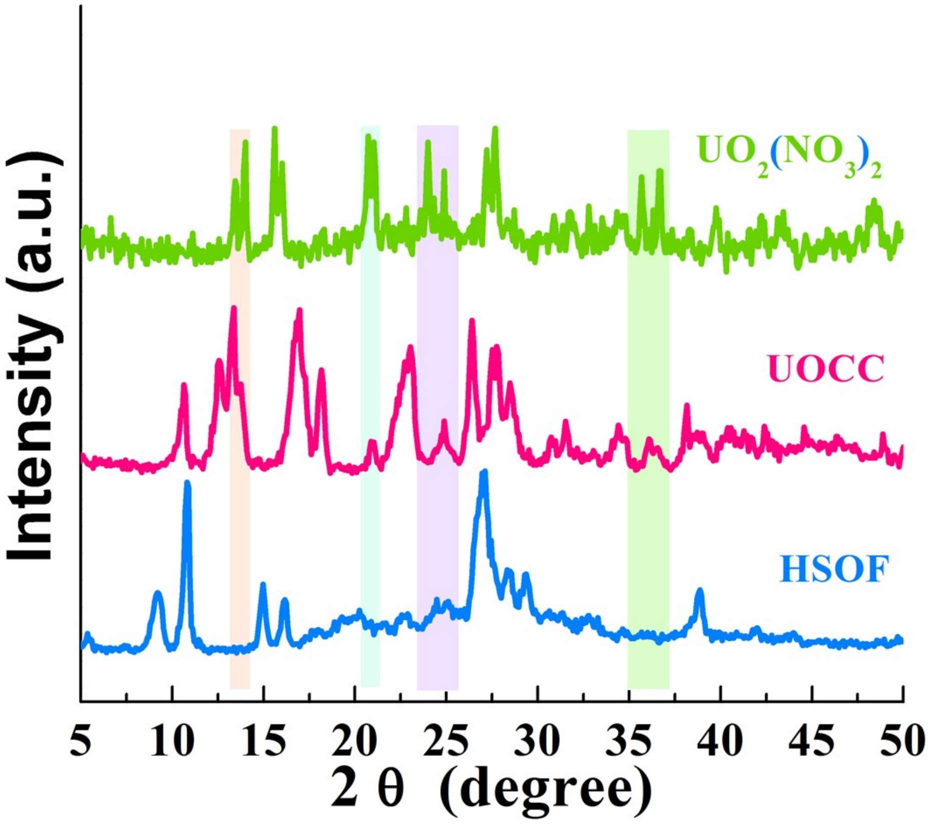

Fig. S4 Powder X-ray diffraction patterns of HSOF, UOCC and $UO_2(NO_3)_2 \cdot 6H_2O$.

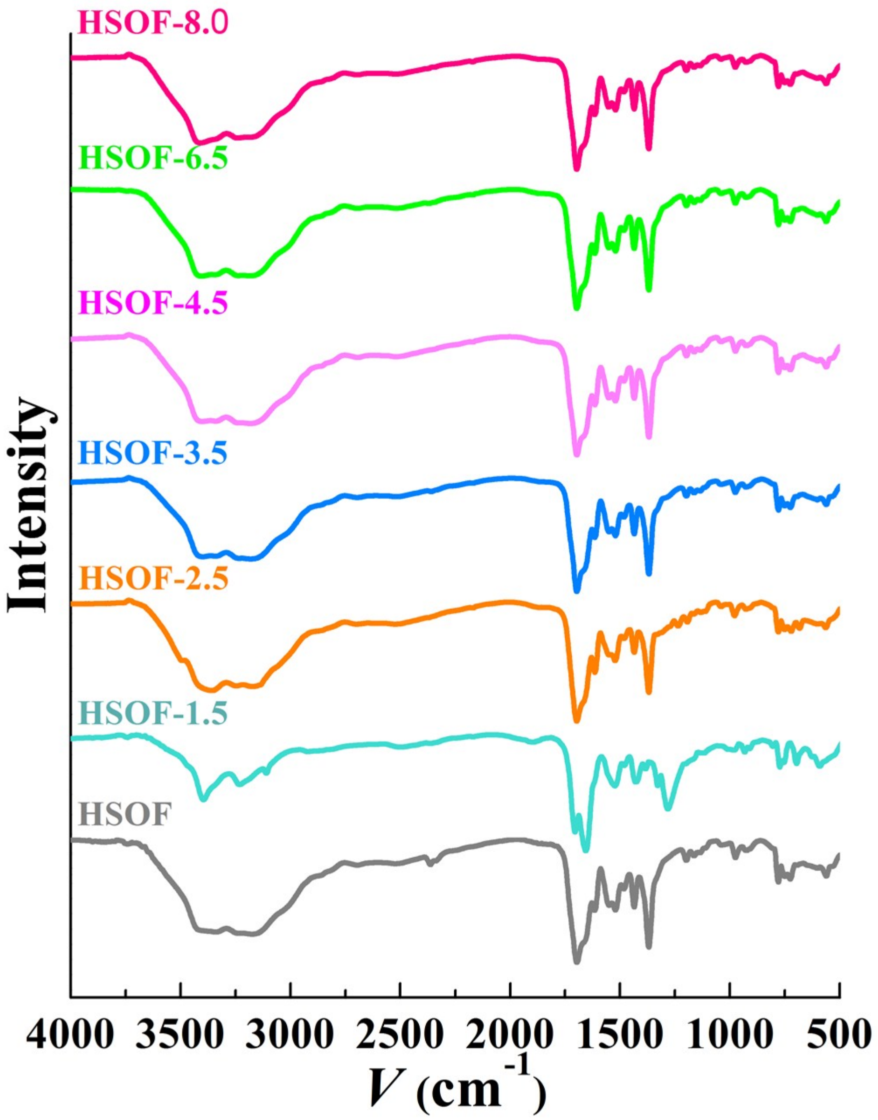

Fig. S5 FT-IR spectra of HSOF materials after treatment in different pH solution. A certain amount of HSOF was added to 50 mL aqueous solution at different pH (1.5, 2.5, 3.5, 4.5, 6.5, 8.0) and stirred 24 h. The as prepared materials were donated as HSOF-1.5, HSOF-2.5, HSOF-3.5, HSOF-4.5, HSOF-6.5, and HSOF-8.0 respectively.

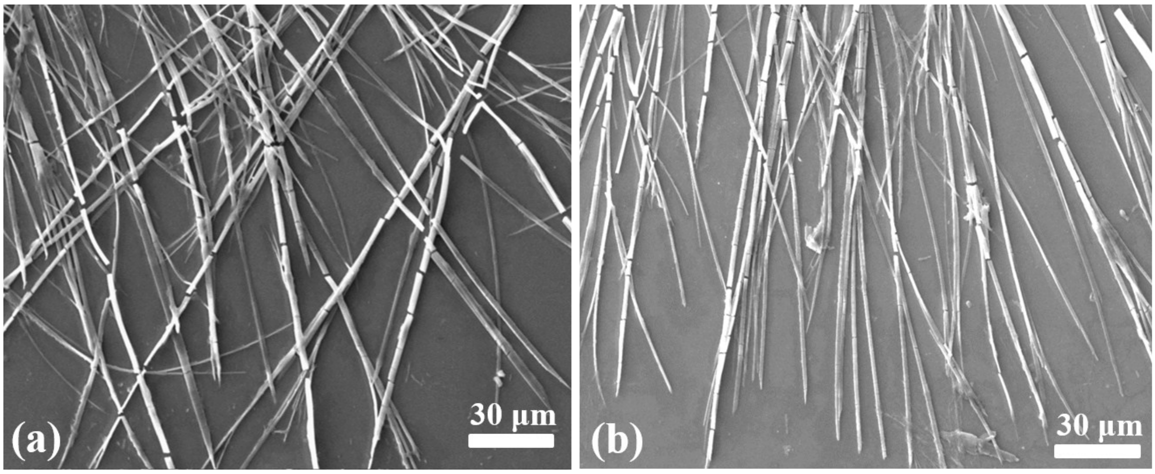

Fig. S6 SEM images of HSOF materials after treatment in different pH solution. (a) pH = 2.5, (b) pH = 4.5.

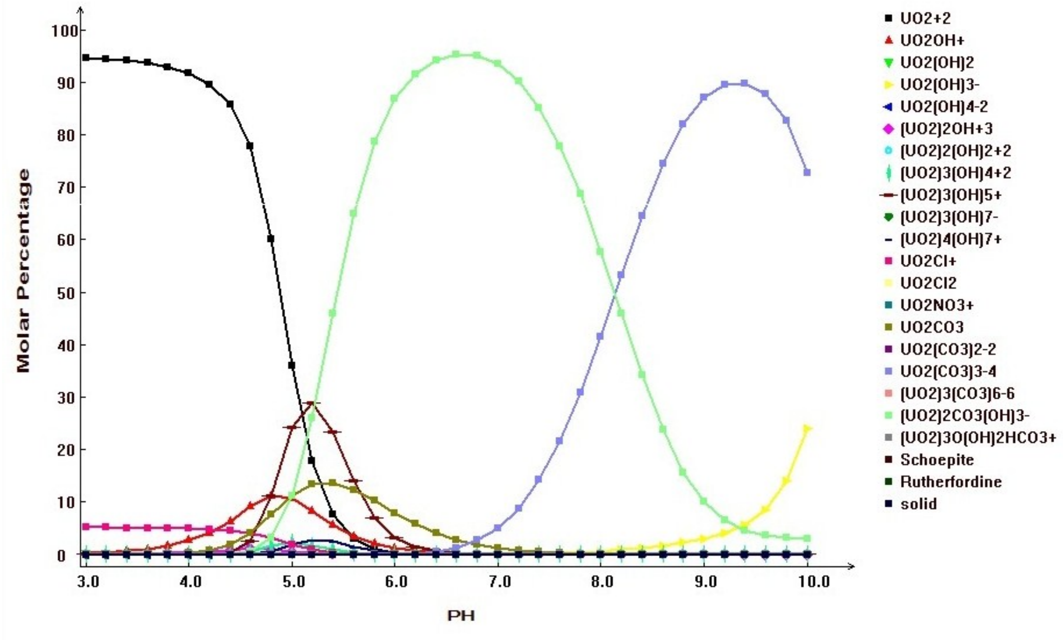

Fig. S7 Distribution of U(VI) species in aqueous solution with a total concentration of 300 mg L^{-1} and pH values ranging from 3 to 10. Calculated by using a CHEMSPEC (C++) program.

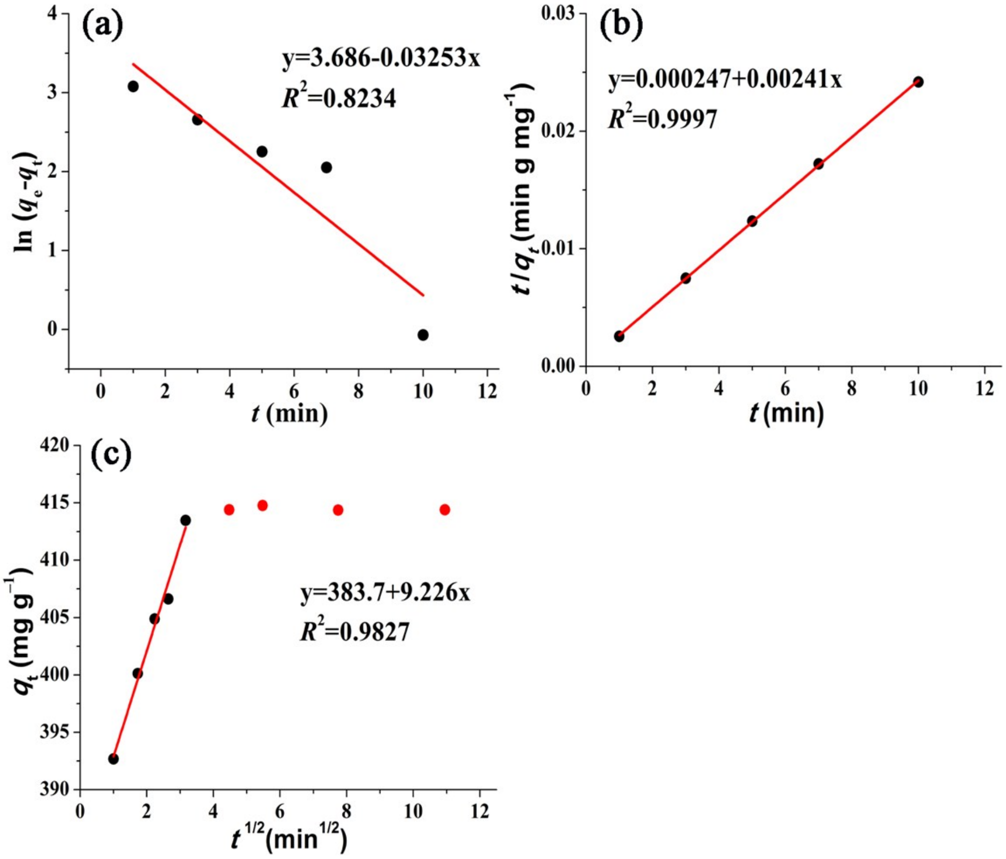

Fig. S8 (a) Pseudo-first-order, (b) pseudo-second-order and (c) intraparticle diffusion model plots for the extraction of U(VI) onto HSOF.

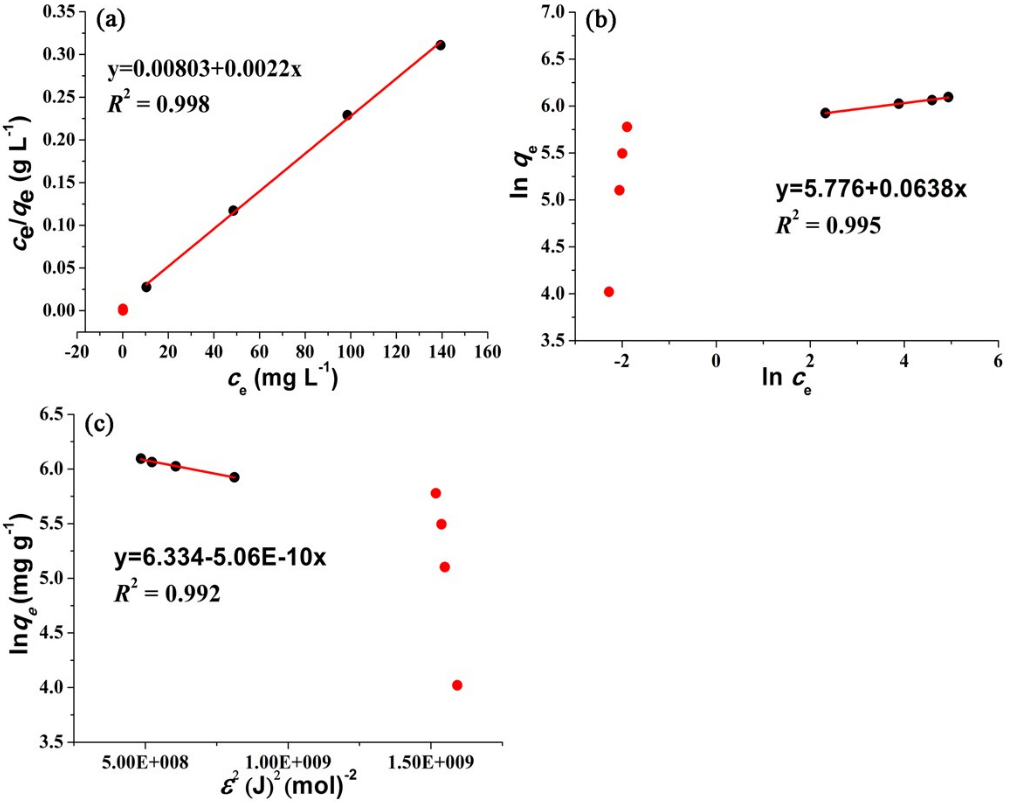

Fig. S9 (a) Langmuir, (b) Freundlich and (c) D-R isotherms for the extraction of U(VI) onto HSOF.

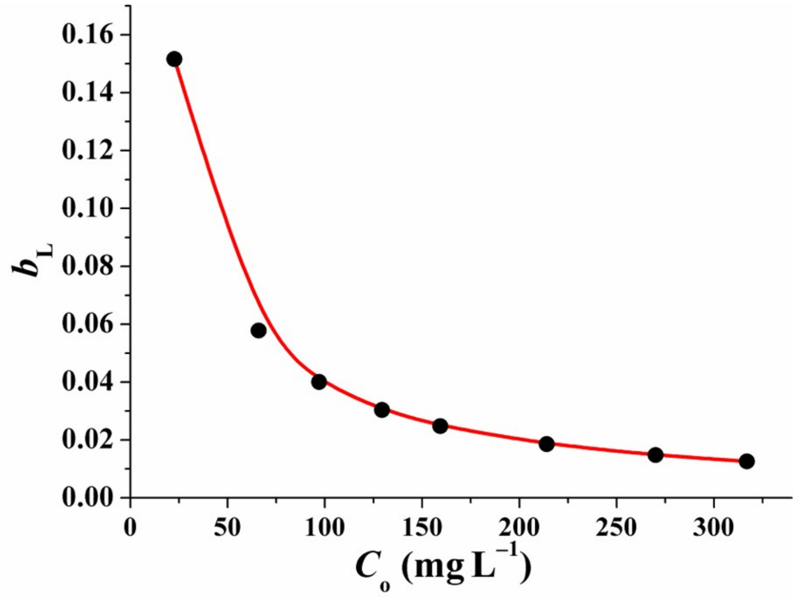

Fig. S10 Langmuir separation factor (pH = 4.5. t = 120 min, v = 25 mL, T = 298 K, and ω = 10 mg).

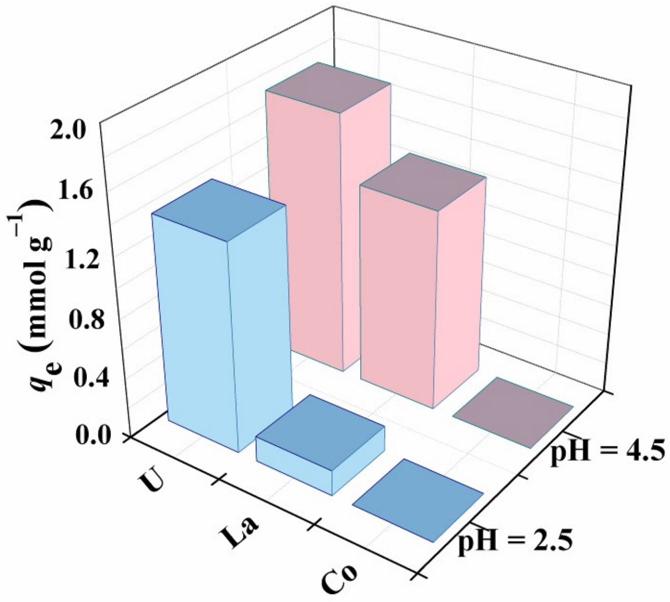

Fig. S11 Effect of pH on the extraction of U(VI), La(III) and Co(II) onto HSOF at different pH in pure metal ion system. ($C_0 \approx 1.0$ mmol L^{-1}, $t = 120$ min, $v = 25$ mL, $T = 298$ K, and $\omega = 10$ mg).

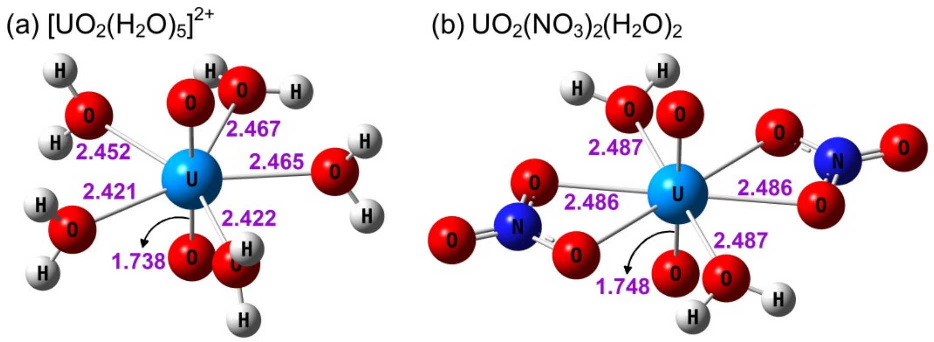
(a) $[UO_2(H_2O)_5]^{2+}$

(b) $UO_2(NO_3)_2(H_2O)_2$

Fig. S12 The optimized structures of the stationary points for (a) $[UO_2(H_2O)_5]^{2+}$ and (b) $UO_2(NO_3)_2(H_2O)_2$ by DFT calculations. The important bond lengths (angstrom) are also shown in this figure.

Reference

1. C. R. Preetha, J. M. Gladis, T. P. Rao and G. Venkateswaran, *Environ. Sci. Technol.* , 2006, **40**, 3070-3074.
2. F. C. Wu, R.-L. Tseng and R. S. Juang, *Water Res.* , 2001, **35**, 613-618.
3. R. L. Tseng, F. C. Wu and R. S. Juang, *Carbon*, 2003, **41**, 487-495.
4. S. Veli and B. Alyüz, *J. Hazard. Mater.*, 2007, **149**, 226-233.
5. J. Perić, M. Trgo and N. Vukojević Medvidović, *Water Res.* , 2004, **38**, 1893-1899.
6. B. Li, L. Ma, Y. Tian, X. D. Yang, J. Li, C. Y. Bai, X. Y. Yang, S. Zhang, S. J. Li and Y. D. Jin, *J. Hazard. Mater.*, 2014, **271**, 41-49.
7. C. A. Başar, *J. Hazard. Mater.*, 2006, **135**, 232-241.
8. E. Oguz, *Physicochem. Eng. Aspects* 2005, **252**, 121-128.
9. S. Zhang, X. Zhao, B. Li, C. Bai, Y. Li, L. Wang, R. Wen, M. Zhang, L. Ma and S. Li, *J. Hazard. Mater.*, 2016, **314**, 95-104.
10. Z. Chen, Z. Zhuang, Q. Cao, X. Pan, X. Guan and Z. Lin, *ACS Appl. Mater. Interfaces*, 2014, **6**, 1301-1305.
11. W. T. Yang, Z. Q. Bai, W. Q. Shi, L. Y. Yuan, T. Tian, Z. F. Chai, H. Wang and Z. M. Sun, *Chem. Commun.*, 2013, **49**, 10415-10417.
12. Z. Q. Bai, L. Y. Yuan, L. Zhu, Z. R. Liu, S. Q. Chu, L. R. Zheng, J. Zhang, Z. F. Chai and W. Q. Shi, *J. Mater. Chem. A*, 2015, **3**, 525-534.
13. L. Y. Yuan, Y.-L. Liu, W.-Q. Shi, Y.-L. Lv, J.-H. Lan, Y.-L. Zhao and Z.-F. Chai, *Dalton Trans.*, 2011, **40**, 7446-7453.
14. H. Wang, L. Ma, K. Cao, J. Geng, J. Liu, Q. Song, X. Yang and S. Li, *J. Hazard. Mater.*, 2012, **229–230**, 321-330.
15. Q. Song, L. Ma, J. Liu, C. Bai, J. Geng, H. Wang, B. Li, L. Wang and S. Li, *J. Colloid Interface Sci.*, 2012, **386**, 291-299.
16. L. Y. Yuan, Y. L. Liu, W. Q. Shi, Z. J. Li, J. H. Lan, Y.-X. Feng, Y. L. Zhao, Y. L. Yuan and Z. F. Chai, *J. Mater. Chem.*, 2012, **22**, 17019-17026.